# *Ab initio* Study on Enantioselective Reduction of Ketones Catalyzed by Thiazolidino[3,4-*c*]oxazaborolidines

LI, Ming*,[a](李明) XIE, Ru-Gang[b](谢如刚) TIAN, An-Min[b](田安民)
[a] *Department of Chemistry, Southwest Normal University, Chongqing 400715, China*
[b] *Department of Chemistry, Sichuan University, Chengdu, Sichuan 610064, China*

**The *ab initio* molecular orbital method is employed to study the enantioselective reduction of acetophenone with borane catalyzed by thiazolidino[3,4-*c*]oxazaborolidine. Computation result shows that the controlling step for the reduction is the decomposition of the catalyst-alkoxyborane adduct and the reduction leads to *S*-alcohols. The transition state of the hydride transfer from the borane moiety to the carbonyl carbon of acetophenone is a twisted chair structure with a B(2)—N(3)—$B_{BH_3}$—$H_{BH_3}$—$C_{CO}$—$O_{CO}$ 6-membered ring.**

**Keywords** *ab initio*, thiazolidino[3,4-*c*]oxazaborolidine, enantioselective reduction of acetophenone, transition state

## Introduction

Thiazolidino[3,4-*c*]oxazaborolidine, as a catalyst, is used in the enantioselective reduction of prochiral ketones.[1-4] As shown in the experiment by Li and Xie,[1] the chirality of reduced products catalyzed by thiazolidino[3,4-*c*]oxazaborolidine is opposite to those by the usual catalyst. This is an interesting work not only for synthetic chemistry but also for theoretical chemistry. In our previous work,[5,6] the structures of the intermediate states for the enantioselective reduction of acetophenone with borane catalyzed by thiazolidino[3,4-*c*]oxazaborolidine were investigated by means of the *ab initio* moleculer orbital method at the 6-31G(d) level. The aim of the present work is to study the transition states for this reduction and the mechanism of the reduction.

## Computations and results

According to the mechanism of the enantioselective reduction of prochiral ketones with borane catalyzed by the usual catalyst suggested by Corey *et al.*,[7] the enantioselective reduction of acetophenone with borane catalyzed by thiazolidino[3,4-*c*]oxazaborolidine mainly involves the steps illustrated in Fig. 1. As presented in Fig. 1, this reduction goes mainly through the transition states **TS1**, **TS2** and **TS3**. The intermediate states **3**, **4**, and the transition states **TS1**, **TS2** and **TS3** involve, respectively, four plausible structures. In the present work, the Hartree-Fock *ab initio* molecular orbital method is used. All the transition states are optimized completely at the HF/6-31G(d) level, and their vibrational analysis and natural bond orbital (NBO) analysis[8,9] are performed at the same computational level. The optimized structures of the transition states are illustrated in Figs. 2, 3, and 4 respectively. Total energies $E$ corrected from zero-point energy, activating energies $\Delta E^{\neq}$, and the first two vibrational frequencies $\nu_1$ and $\nu_2$ for all the transition states are summarized in Table 1. Selected bond lengths and corresponding Mulliken overlap populations are shown in Table 2. For easy discussion, the results for the catalyst **1**, the catalyst-borane adduct **2**, the catalyst-borane-acetophenone adduct **3**, and the catalyst-alkoxyborane adduct **4** are also listed in Tables 1 and 2.

* E-mail: shilm@swnu.edu.cn
Received April 15, 2002; revised July 3, 2002; accepted August 12, 2002.
Project supported by the Science Foundation of National Education Ministry (No. 99106).

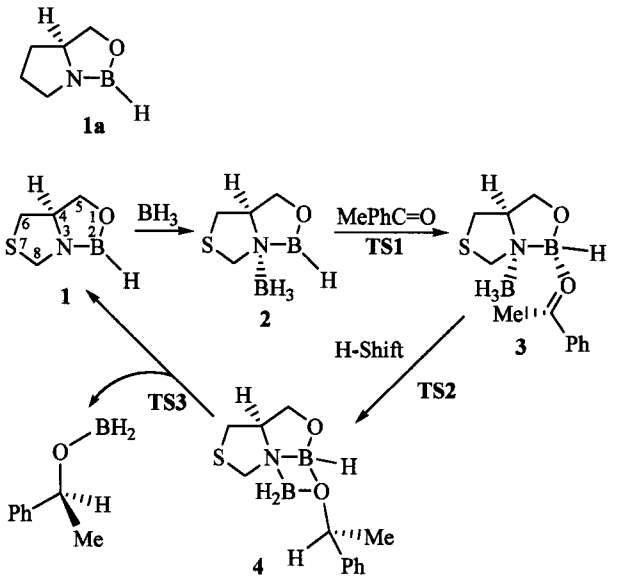


**Fig. 1** Enantioselective reduction of acetophenone with borane catalyzed by thiazolidino[3,4-*c*]oxazaborolidine.

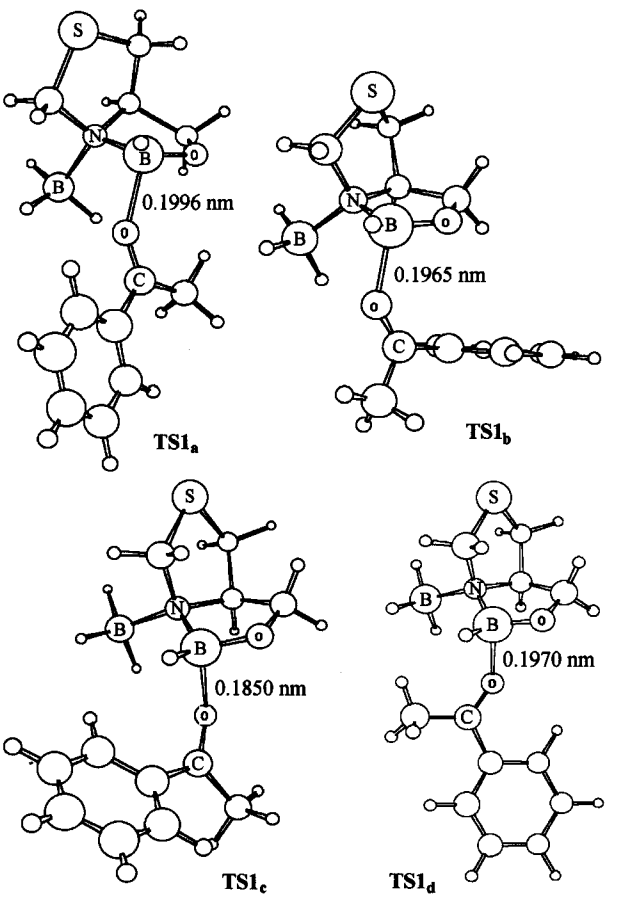


**Fig. 2** Optimized structures of the transition states $\mathbf{TS1_a}$, $\mathbf{TS1_b}$, $\mathbf{TS1_c}$ and $\mathbf{TS1_d}$.

## Discussion

*Structures of transition states*

The transition state **TS1** for the formation of the adduct **3** involves four structures, $\mathbf{TS1_a}$, $\mathbf{TS1_b}$, $\mathbf{TS1_c}$ and $\mathbf{TS1_d}$. The optimized structures of these transition states are illustrated in Fig. 2. As shown in Table 1, they have a sole imaginary frequency. The distances between the carbonyl oxygen $O_{CO}$ of acetophenone and B(2) of the catalyst **1** in these transition states are 0.1996 nm for $\mathbf{TS1_a}$, 0.1965 nm for $\mathbf{TS1_b}$, 0.1850 nm for $\mathbf{TS1_c}$ and 0.1970 nm for $\mathbf{TS1_d}$, and the corresponding Mulliken overlap populations are 0.048, 0.045, 0.053, and 0.050 respectively. The $O_{CO}$-B(2)-N(3) angles and the $O_{CO}$-B(2)-N(3)-C(4) torsion angles are, respectively, 107.0° and 139.8° for $\mathbf{TS1_a}$, 107.6° and 105.2° for $\mathbf{TS1_b}$, 103.4° and 77.3° for $\mathbf{TS1_c}$, and 104.7° and 77.2° for $\mathbf{TS1_d}$. The $C_{CO}$-$O_{CO}$-B(2) angles and the $C_{CO}$-$O_{CO}$-B(2)-N(3) torsion angles are 141.9° and −102.2° for $\mathbf{TS1_a}$, 139.8° and −103.0° for $\mathbf{TS1_b}$, 134.9° and 145.1° for $\mathbf{TS1_c}$, and 133.4° and 112.8° for $\mathbf{TS1_d}$. The carbonyl bonds are longer than the $C_{CO}$—$O_{CO}$ bond of free acetophenone and shorter than those of the adducts **3a**, **3b**, **3c** and **3d** (Table 2). It is clear that the $C_{CO}$—$O_{CO}$ bonds in these transition states are weakened, compared with the $C_{CO}$—$O_{CO}$ bond of free acetophenone.

As demonstrated by the natural bond orbital (NBO) analysis, the stabilization interaction energies $E(2)$ between lone electron pairs of $O_{CO}$ and the empty orbital of B(2) in $\mathbf{TS1_a}$, $\mathbf{TS1_b}$, $\mathbf{TS1_c}$ and $\mathbf{TS1_d}$ are 410.6, 404.1, 550.0 and 418.3 kJ/mol respectively. In the NBO analysis, the stabilization interaction energies $E(2)$ are used to describe the delocalization trend of electrons from a donor to an acceptor. It is clear that in $\mathbf{TS1_a}$, $\mathbf{TS1_b}$, $\mathbf{TS1_c}$ and $\mathbf{TS1_d}$, there are notable interactions between $O_{CO}$ and B(2) because of the large stabilization interaction energies between lone electron pairs of $O_{CO}$ and the empty p orbital of B(2).

The transition state **TS2** for the hydride transfer from the borane moiety to the carbonyl carbon of acetophenone also involves four structures, $\mathbf{TS2_a}$, $\mathbf{TS2_b}$, $\mathbf{TS2_c}$ and $\mathbf{TS2_d}$. Their optimized structures are presented in Fig. 3. The imaginary frequencies for these transition states are sole. The $B_{BH_3}$—$H_{BH_3}$ and $C_{CO}$—$O_{CO}$ bond lengths and their Mulliken overlap populations for these transition

**Table 1** Total energies $E$ (a.u.), formation energies $\Delta E$ (kJ/mol), activating energies $\Delta E^{\neq}$ (kJ/mol), and vibrational frequencies $\nu$ ($cm^{-1}$)

| | $E$ | $\Delta E$ | $\Delta E^{\neq}$ | $\nu_1$ | $\nu_2$ |
|---|---|---|---|---|---|
| $BH_3$ | -26.3617 | | | | |
| PhMeCO | -382.3268 | | | | |
| $PhMeCHOBH_2$ | -408.7472 | | | | |
| **1** | -707.5675 | | | 89.0 | 141.5 |
| **2** | -733.9398 | -27.83 | | 31.1 | 136.5 |
| **3a** | -1116.2568 | 25.73 | | 29.2 | 34.8 |
| **3b** | -1116.2520 | 38.33 | | 20.6 | 33.6 |
| **3c** | -1116.2544 | 32.03 | | 33.0 | 38.5 |
| **3d** | -1116.2595 | 18.64 | | 27.9 | 34.3 |
| **4a** | -1116.3124 | -145.98 | | 29.6 | 36.3 |
| **4b** | -1116.3114 | -155.95 | | 29.6 | 32.0 |
| **4c** | -1116.3125 | -152.54 | | 23.8 | 36.3 |
| **4d** | -1116.3111 | -135.48 | | 19.1 | 27.5 |
| $TS1_a$ | -1116.2556 | | 28.88 | -106.2 | 23.2 |
| $TS1_b$ | -1116.2446 | | 57.76 | -98.8 | 22.8 |
| $TS1_c$ | -1116.2536 | | 34.13 | -92.7 | 37.3 |
| $TS1_d$ | -1116.2567 | | 25.99 | -100.9 | 19.5 |
| $TS2_a$ | -1116.2412 | | 38.33 | -658.6 | 26.0 |
| $TS2_b$ | -1116.2396 | | 32.56 | -570.0 | 41.0 |
| $TS2_c$ | -1116.2421 | | 27.04 | -512.8 | 44.2 |
| $TS2_d$ | -1116.2455 | | 36.76 | -591.9 | 34.4 |
| $TS3_a$ | -1116.3009 | | 30.19 | -25.8 | 13.8 |
| $TS3_b$ | -1116.3005 | | 28.62 | -26.8 | 22.4 |
| $TS3_c$ | -1116.3016 | | 28.62 | -21.8 | 6.6 |
| $TS3_d$ | -1116.3024 | | 22.84 | -22.3 | 15.6 |

**Table 2** Selected bond lengths (nm) and corresponding Mulliken overlap populations (in parentheses)

| | $B_{BH_3}—H_{BH_3}$ | $N(3)—B_{BH_3}$ | $O_{CO}—B(2)$ | $C_{CO}—O_{CO}$ | $C_{CO}—H_{BH_3}$ | $O_{CO}—B_{BH_3}$ |
|---|---|---|---|---|---|---|
| $BH_3$ | 0.1188 (0.413) | | | | | |
| PhMeCO | | | | 0.1196 (0.599) | | |
| **2** | 0.1210 (0.414) | 0.1717 (0.118) | | | | |
| **3a** | 0.1218 (0.401) | 0.1664 (0.173) | 0.1581 (0.129) | 0.1227 (0.418) | 0.2782 (0.003) | 0.2843 |
| **3b** | 0.1217 (0.409) | 0.1676 (0.166) | 0.1633 (0.092) | 0.1223 (0.442) | 0.2785 (0.005) | 0.2830 |
| **3c** | 0.1218 (0.401) | 0.1660 (0.173) | 0.1734 (0.058) | 0.1216 (0.470) | 0.3291 (0.002) | 0.3016 |
| **3d** | 0.1217 (0.409) | 0.1656 (0.176) | 0.1644 (0.081) | 0.1223 (0.449) | 0.2829 (0.005) | 0.3007 |
| **4a** | | 0.1613 (0.203) | 0.1567 (0.135) | 0.1426 (0.145) | | 0.1548 (0.188) |

Continued

| | $B_{BH_3}$—$H_{BH_3}$ | N(3)—$B_{BH_3}$ | $O_{CO}$—B(2) | $C_{CO}$—$O_{CO}$ | $C_{CO}$—$H_{BH_3}$ | $O_{CO}$—$B_{BH_3}$ |
|---|---|---|---|---|---|---|
| **4b** | | 0.1607 | 0.1568 | 0.1426 | | 0.1546 |
| | | (0.211) | (0.132) | (0.147) | | (0.193) |
| **4c** | | 0.1600 | 0.1571 | 0.1427 | | 0.1547 |
| | | (0.209) | (0.122) | (0.144) | | (0.189) |
| **4d** | | 0.1610 | 0.1563 | 0.1422 | | 0.1533 |
| | | (0.207) | (0.129) | (0.148) | | (0.195) |
| **TS1$_a$** | 0.1209 | 0.1709 | 0.1996 | 0.1207 | 0.3061 | 0.2952 |
| | (0.412) | (0.141) | (0.048) | (0.482) | | |
| **TS1$_b$** | 0.1208 | 0.1694 | 0.1965 | 0.1201 | 0.3063 | 0.2970 |
| | (0.409) | (0.148) | (0.045) | (0.507) | | |
| **TS1$_c$** | 0.1209 | 0.1666 | 0.1850 | 0.1212 | 0.3431 | 0.3078 |
| | (0.417) | (0.165) | (0.053) | (0.482) | | |
| **TS1$_d$** | 0.1209 | 0.1669 | 0.1970 | 0.1211 | 0.3201 | 0.3179 |
| | (0.416) | (0.160) | (0.050) | (0.486) | | |
| **TS2$_a$** | 0.1284 | 0.1599 | 0.1495 | 0.1278 | 0.1626 | 0.2723 |
| | (0.264) | (0.216) | (0.220) | (0.295) | (0.144) | |
| **TS2$_b$** | 0.1275 | 0.1594 | 0.1532 | 0.1265 | 0.1660 | 0.2789 |
| | (0.271) | (0.227) | (0.183) | (0.334) | (0.141) | |
| **TS2$_c$** | 0.1269 | 0.1601 | 0.1551 | 0.1262 | 0.1680 | 0.2921 |
| | (0.277) | (0.225) | (0.151) | (0.361) | (0.125) | |
| **TS2$_d$** | 0.1281 | 0.1593 | 0.1530 | 0.1269 | 0.1624 | 0.2898 |
| | (0.280) | (0.230) | (0.164) | (0.352) | (0.143) | |
| **TS3$_a$** | | 0.1700 | 0.2299 | 0.1397 | | 0.1450 |
| | | (0.129) | (0.047) | (0.213) | | (0.281) |
| **TS3$_b$** | | 0.1715 | 0.2291 | 0.1399 | | 0.1447 |
| | | (0.121) | (0.045) | (0.207) | | (0.289) |
| **TS3$_c$** | | 0.1690 | 0.2416 | 0.1400 | | 0.1448 |
| | | (0.133) | (0.046) | (0.211) | | (0.292) |
| **TS3$_d$** | | 0.1706 | 0.2371 | 0.1398 | | 0.1450 |
| | | (0.125) | (0.050) | (0.209) | | (0.282) |

states are shown in Table 2. It is obvious that compared with free acetophenone or the adduct **3**, these transition states involve longer and weaker $B_{BH_3}$—$H_{BH_3}$ and $C_{CO}$—$O_{CO}$ bonds. The interactions between $C_{CO}$ and $H_{BH_3}$ in the transition states are strengthened greatly and the $C_{CO}$—$H_{BH_3}$ distances are decreased considerably, compared with the $C_{CO}$—$H_{BH_3}$ distances and their Mulliken overlap populations in the adduct **3**. The considerable shortening of the $C_{CO}$—$H_{BH_3}$ distance results in the formation of a B(2)—N(3)—$B_{BH_3}$—$H_{BH_3}$—$C_{CO}$—$O_{CO}$ 6-membered ring in each of the transition states. By inspection of the structures of the transition states, it is found that both **TS2$_a$** and **TS2$_b$** involve a twisted boat structure, whereas the transition states **TS2$_c$** and **TS2$_d$** involve a twisted chair structure. Both the twisted boat and the twisted chair structures consist of the B(2)—N(3)—$B_{BH_3}$—$H_{BH_3}$—$C_{CO}$—$O_{CO}$ 6-membered ring and the oxazaborolidine ring. In addition, as illustrated in Fig. 3, the hydride of the borane moiety in **TS2$_a$** and **TS2$_c$** can, in geometry, attack the *Si* plane of acetophenone, which ought to result in *S*-alcohols, and that in **TS2$_b$** and **TS2$_d$** can attack the *Re* plane of acetophenone, which ought to lead to *R*-alcohols. Therefore, the reduced products determined by **TS2$_a$** and **TS2$_c$** are *S*-alcohols, whereas those determined by **TS2$_b$** and **TS2$_d$** are *R*-alcohols.

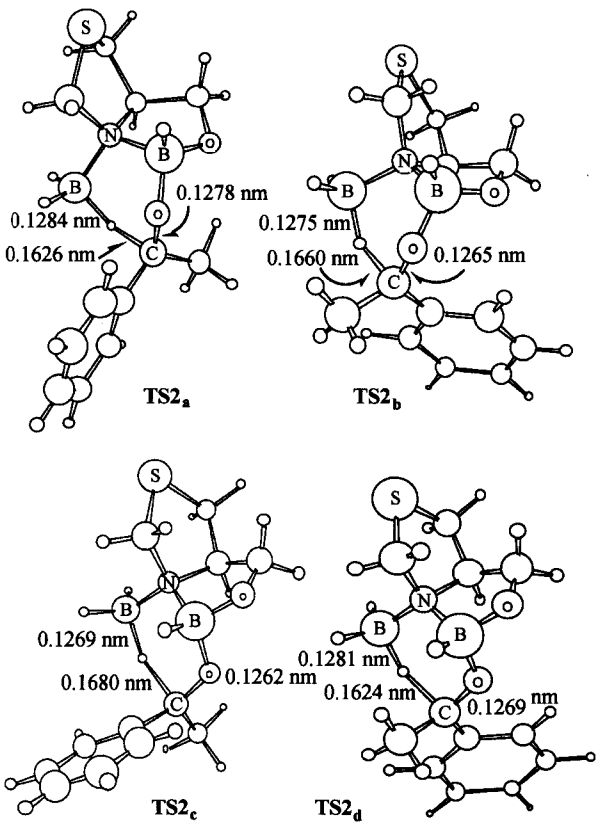


**Fig. 3** Optimized structures of the transition states $TS2_a$, $TS2_b$, $TS2_c$ and $TS2_d$.

It is illustrated by the NBO analysis of the transition states that the stabilization interaction energies $E(2)$ between $p_\pi$ lone electron pairs of $O_{CO}$ and the empty $p_\pi$ orbital of $C_{CO}$ are 435.3 kJ/mol for $TS2_a$, 465.1 kJ/mol for $TS2_b$, 503.7 kJ/mol for $TS2_c$ and 474.1 kJ/mol for $TS2_d$. It is obvious that there are notable interactions between the $p_\pi$ orbitals of $O_{CO}$ and $C_{CO}$ in the transition states. The existence of the great interactions implies that there are weak $\pi$ carbonyl bonds. Furthermore, $E(2)$ between the $B_{BH_3}$—$H_{BH_3}$ bonding orbital and the empty p orbital of $C_{CO}$ are 576.4 kJ/mol for $TS2_a$, 485.7 kJ/mol for $TS2_b$, 431.7 kJ/mol for $TS2_c$ and 552.2 kJ/mol for $TS2_d$. These results imply that there are quite strong interactions between $H_{BH_3}$ and $C_{CO}$ in $TS2_a$, $TS2_b$, $TS2_c$ and $TS2_d$, which is in agreement with the above conclusion.

$TS3_a$, $TS3_b$, $TS3_c$ and $TS3_d$ are four stable structures of the transition state **TS3**. Their optimized structures are shown in Fig. 4. Their imaginary frequencies are sole. By comparison with the adduct **4**, the most notable feature of these transition states is the increase in the $O_{CO}$—B(2) distances. As illustrated in Table 2, the $O_{CO}$—B(2) distances are 0.2299 nm for $TS3_a$, 0.2291 nm for $TS3_b$, 0.2416 nm for $TS3_c$ and 0.2371 nm for $TS3_d$, and their Mulliken overlap populations are decreased from about 0.13 of the adduct **4** to about 0.05 of the transition states. The B—O—B—N 4-membered rings in these transition states are twisted by about 20° (in the adduct **4**, these 4-membered rings are almost plane). In addition, the N(3)—$B_{BH_3}$ bond lengths in the transition states are increased a little and the $O_{CO}$—$B_{BH_3}$ bonds are shortened. Further, the stabilization interaction energies $E(2)$ between lone electron pairs of $O_{CO}$ and the empty orbital of B(2) for $TS3_a$, $TS3_b$, $TS3_c$ and $TS3_d$ are 140.3, 146.7, 91.8, and 112.1 kJ/mol respectively. Obviously, these $E(2)$ are small and thus the interactions between $O_{CO}$ and B(2) are weak.

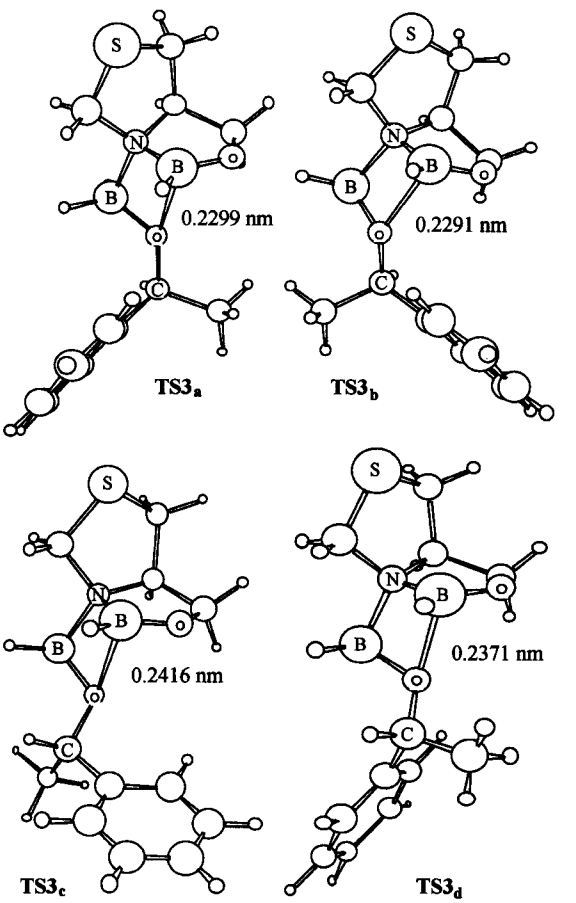


**Fig. 4** Optimized structures of the transition states $TS3_a$, $TS3_b$, $TS3_c$ and $TS3_d$.

*Enantioselective reduction of acetophenone*

As demonstrated above, the transition states **TS1**, **TS2** and **TS3** involve, respectively, four structures. In our previous work,[5,6] it has been shown that the adduct **3** and the adduct **4** have also four stable structures individually. Therefore, the enantioselective reduction of acetophenone with borane catalyzed by catalyst **1** involves four reaction paths: **1**→**2**→$\mathbf{TS1_a}$→**3a**→$\mathbf{TS2_a}$→**4a**→$\mathbf{TS3_a}$→$PhMeCHOBH_2$, **1**→**2**→$\mathbf{TS1_b}$→**3b**→$\mathbf{TS2_b}$→**4b**→$\mathbf{TS3_b}$→$PhMeCHOBH_2$, **1**→**2**→$\mathbf{TS1_c}$→**3c**→$\mathbf{TS2_c}$→**4c**→$\mathbf{TS3_c}$→$PhMeCHOBH_2$, and **1**→**2**→$\mathbf{TS1_d}$→**3d**→$\mathbf{TS2_d}$→**4d**→$\mathbf{TS3_d}$→$PhMeCHOBH_2$. As indicated above, the first path and the third path determine *S*-alcohols, while the second path and the fourth path determine *R*-alcohols.

As shown in Table 1, the activating energies $\Delta E^{\neq}$ of the transition states $\mathbf{TS1_a}$, $\mathbf{TS2_a}$ and $\mathbf{TS3_a}$ are, respectively, 28.88, 38.33 and 30.19 kJ/mol. It is clear that in this path, the controlling step for the enantioselective reduction is the hydride transfer from the borane moiety to the carbonyl carbon of acetophenone because of its largest activating energy. $\Delta E^{\neq}$ of $\mathbf{TS1_b}$, $\mathbf{TS2_b}$ and $\mathbf{TS3_b}$ are 57.76, 32.56 and 28.62 kJ/mol respectively. The controlling step for this path is the formation of the adduct **3**. $\Delta E^{\neq}$ of $\mathbf{TS1_c}$, $\mathbf{TS2_c}$ and $\mathbf{TS3_c}$ are 34.13, 27.04 and 28.62 kJ/mol respectively. The controlling step for this path is also the formation of the adduct **3**. $\Delta E^{\neq}$ of $\mathbf{TS1_d}$, $\mathbf{TS2_d}$ and $\mathbf{TS3_d}$ are 25.99, 36.76 and 22.84 kJ/mol respectively. The controlling step for this path is also the hydride transfer from the borane moiety to the carbonyl carbon. In summary, the activating energies of the controlling steps for these four reduction paths are 38.33 kJ/mol for $\mathbf{TS2_a}$, 57.76 kJ/mol for $\mathbf{TS1_b}$, 34.13 kJ/mol for $\mathbf{TS1_c}$ and 36.76 kJ/mol for $\mathbf{TS2_d}$. It is obvious that the third reduction path has the lowest activating energy for the controlling step among these four reduction paths. Therefore, the reduced products are generated mainly through the third path. According to the above discussion, the main reduced products are *S*-alcohols. The present theoretical result is in agreement with the experiment by Li and Xie.[1] It must be emphasized that the fourth reduction path has also low activating energy (36.76 kJ/mol) for the controlling step and thus *R*-alcohols may be generated during the enantioselective reduction of acetophenone. Fig. 5 shows the energy relationship of the enantioselective reduction of acetophenone with borane catalyzed by **1**. In addition, it is shown from Table 1 that the enantioselective reduction of acetophenone with borane catalyzed by catalyst **1** is exothermic.

As indicated above, the transition state $\mathbf{TS2_c}$ in the third reduction path has a twisted chair structure that

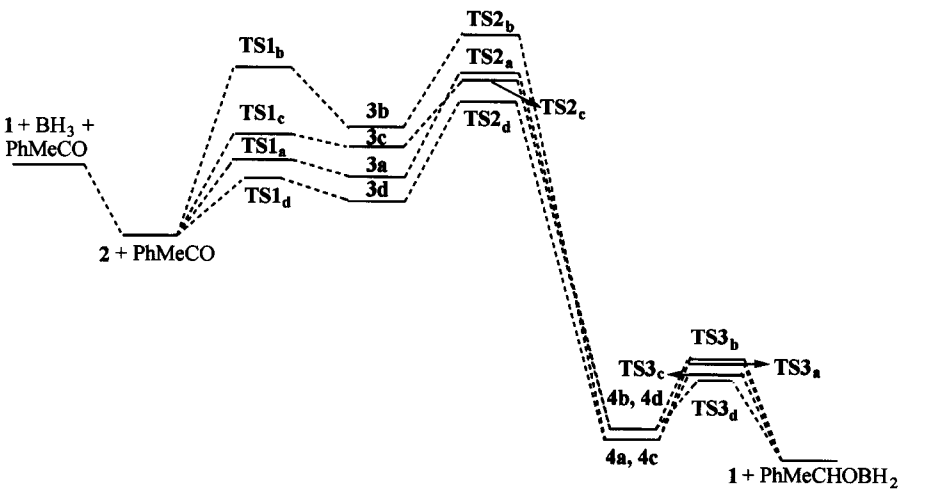


$\Delta E^{\neq}(\mathbf{TS1_a}) = 28.88$ kJ/mol $\Delta E^{\neq}(\mathbf{TS1_b}) = 57.76$ kJ/mol $\Delta E^{\neq}(\mathbf{TS1_c}) = 34.13$ kJ/mol $\Delta E^{\neq}(\mathbf{TS1_d}) = 25.99$ kJ/mol

$\Delta E^{\neq}(\mathbf{TS2_a}) = 38.33$ kJ/mol $\Delta E^{\neq}(\mathbf{TS2_b}) = 32.56$ kJ/mol $\Delta E^{\neq}(\mathbf{TS2_c}) = 27.04$ kJ/mol $\Delta E^{\neq}(\mathbf{TS2_d}) = 36.67$ kJ/mol

$\Delta E^{\neq}(\mathbf{TS3_a}) = 30.19$ kJ/mol $\Delta E^{\neq}(\mathbf{TS3_b}) = 28.62$ kJ/mol $\Delta E^{\neq}(\mathbf{TS3_c}) = 28.62$ kJ/mol $\Delta E^{\neq}(\mathbf{TS3_d}) = 22.84$ kJ/mol

**Fig. 5** Energy relationship of the enantioselective reduction of acetophenone with borane catalyzed by thiazolidino[3,4-*c*]oxazaborolidine.

consists of the B(2)—N(3)—$B_{BH_3}$—$H_{BH_3}$—$C_{CO}$—$O_{CO}$ 6-membered ring and the oxazaborolidine ring. As a result, the transition state of the hydride transfer for the enantioselective reduction of acetophenone with borane catalyzed by catalyst **1** is of a twisted chair structure, which is in agreement with the MNDO result of the usual catalytic system obtained by Jones and Liotta.[10]

Finally, the reduction of acetophenone without thiazolidino[3,4-*c*]oxazaborolidine is computed. The reduction activating energy $\Delta E^{\neq}$ is 59.6 kJ/mol, which is much greater than the activating energies of the reduction catalyzed by **1**. It is clear that the catalytic potentials of thiazolidino[3,4-*c*]oxazaborolidine are considerable.

## Conclusions

In summary, the enantioselective reduction of acetophenone with borane catalyzed by thiazolidino[3,4-*c*] oxazaborolidine is exothermic. The reduction goes mainly through the formation of the catalyst-borane adduct, the catalyst-borane-acetophenone adduct, and the catalyst-alkoxyborane adduct and the decomposition of the catalyst-alkoxyborane adduct with the regeneration of the catalyst. The reduction controlling step is the decomposition of the catalyst-alkoxyborane adduct. The reduction of acetophenone leads to *S*-alcohols, which is in agreement with the experiment. The transition state of the hydride transfer from the borane moiety to the carbonyl carbon of acetophenone has a twisted chair structure with a B(2)—N(3)—$B_{BH_3}$—$H_{BH_3}$—$C_{CO}$—$O_{CO}$ 6-membered ring.

## References


1 Li, X. S.; Xie, R. G. *Tetrahedron: Asymmetry* **1996**, *7*, 2779.

2 Huang, H.-L.; Lin, Y.-C.; Chen, S.-F.; Wang, C.-L. J.; Liu, L.-T. *Tetrahedron: Asymmetry* **1996**, *7*, 3067.

3 Reiners, I.; Martens, J.; Schwarz, S.; Henkel, H. *Tetrahedron: Asymmetry* **1996**, *7*, 1763.

4 Trentmann, W.; Mehler, T.; Martens, J. *Tetrahedron: Asymmetry* **1997**, *8*, 2033.

5 Li, M.; Xie, R. G.; Hu, C. W.; Wang, X.; Tian, A. M. *Int. J. Quantum Chem.* **2000**, *78*, 245.

6 Li, M.; Xie, R. G.; Tian, A. M. *Acta Chim. Sinica* **2000**, *58*, 510 (in Chinese).

7 Corey, E. J.; Bakshi, R. K.; Shibata, S. *J. Am. Chem. Soc.* **1987**, *109*, 5551.

8 Reed, A. E.; Curtiss, L. A.; Weinhold, F. *Chem. Rev.* **1988**, *88*, 899.

9 Reed, A. E.; Weinstock, R. B.; Weinhold, F. *J. Chem. Phys.* **1985**, *83*, 735.

10 Jones, D. K.; Liotta, D. C.; Shinkai, I.; Mathre, D. J. *J. Org. Chem.* **1993**, *58*, 1993.


(E0204152 PAN, B. F.; HUANG, W. Q.)